5426 *Chem. Mater.* **2009,** *21,* 5426–5434
DOI:10.1021/cm902028q

CHEMISTRY OF MATERIALS
Article

Influence of $HSiO_{1.5}$ Sol−Gel Polymer Structure and Composition on the Size and Luminescent Properties of Silicon Nanocrystals

Eric J. Henderson, Joel A. Kelly, and Jonathan G. C. Veinot*

Department of Chemistry, University of Alberta, Edmonton, Alberta, Canada

Received July 6, 2009. Revised Manuscript Received September 25, 2009

We report the preparation of SiO_2-embedded silicon nanocrystals (Si-NCs) from the thermal processing of sol−gel polymers derived from trichlorosilane ($HSiCl_3$). Straightforward addition of water to $HSiCl_3$ generates a cross-linked $(HSiO_{1.5})_n$ sol−gel polymer suitable for the generation of bulk quantities of SiO_2-embedded Si-NCs. It is shown that structural differences between the present $(HSiO_{1.5})_n$ polymer and hydrogen silsesquioxane (HSQ) result in controllable differences in the resulting oxide-embedded Si-NCs produced from these precursors. A polymer structure/NC size relationship is further delineated through the preparation and evaluation of methyl-modified $(HSiO_{1.5})_n(CH_3SiO_{1.5})_m$ ($m \ll n$, $m + n = 1$) sol−gel copolymers, in which a low concentration of methyl groups acts as a polymer network modifier and influences the formation of Si-NCs during thermal processing. Si-NC size is readily tailored by controlled variations to peak processing temperature for $(HSiO_{1.5})_n$ and composition (n and m) for $(HSiO_{1.5})_n(CH_3SiO_{1.5})_m$. Furthermore, the present Si-NCs exhibit size-dependent photoluminescence (PL) in accordance with the principles of quantum confinement. Freestanding Si-NCs are obtained through chemical etching of the oxide matrix and exhibit tunable PL throughout the visible spectrum.

Introduction

Silicon nanocrystals (Si-NCs) are the focus of intense research because of their unique optical and electronic characteristics. The discovery of intense room-temperature photoluminescence (PL) from porous Si (*p*-Si) by Canham[1] almost two decades ago has not only challenged bulk semiconductor band structure models[2,3] but also significantly expanded the potential applications of these Si-based materials, including optoelectronics,[4,5] nonvolatile memory,[6,7] and biological fluorescence imaging.[8] In the bulk, the electronic structure of Si provides an indirect band gap, making the optical transition dipole-forbidden and limiting practical optoelectronic applications because of the resulting low PL intensity and slow carrier dynamics. However, these obstacles can be effectively overcome by reducing the dimensions of the semiconductor crystal to sizes approaching the Bohr exciton radius (ca. 5 nm for Si). In this size regime, quantum confinement effects emerge and PL intensity dramatically increases while blue shifting with decreasing particle size.

We have demonstrated that reductive thermal processing of hydrogen silsesquioxane (HSQ, $H_8Si_8O_{12}$) in 5% H_2/95% Ar is a straightforward method to produce well-defined, luminescent Si-NCs embedded in a SiO_2 matrix.[9,10] During thermal processing, redistribution reactions that are driven by the formation of thermodynamically stable SiO_2 lead to Si atomic diffusion throughout the oxide matrix, the clustering of Si-rich domains, and their crystallization to form Si-NCs. In this HSQ-based preparation, control over Si-NC size is readily achieved through variations to the peak thermal processing temperature. The resulting oxide-embedded Si-NCs exhibit size-dependent intense visible and near-infrared (NIR) PL in accordance with the principles of quantum confinement. The role of quantum confinement in governing the emission process, as opposed to surface, oxide, or interface states, has been confirmed through X-ray excited optical luminescence (XEOL) spectroscopy.[11] In these same investigations, it was also found that extended thermal processing time resulted in a red-shift in PL emission maxima with no change in Si-NC size. These observations were attributed to nonresonant carrier tunnelling to larger nanocrystals which form a minimum in the potential landscape of the system, and whose PL was activated

*Corresponding author. Fax: 780-492-8231. Tel.: 780-492-7206. E-mail: jveinot@ualberta.ca.

(1) Canham, L. T. *Appl. Phys. Lett.* **1990**, *57*, 1046.
(2) Brus, L. *J. Phys. Chem.* **1994**, *98*, 3575.
(3) Alivisatos, A. P. *J. Phys. Chem.* **1996**, *100*, 13226.
(4) Pavesi, L.; Dal Negro, L.; Mazzoleni, C.; Franzò, G.; Priolo, F. *Nature* **2000**, *408*, 440.
(5) Walters, R. J.; Bourianoff, G. I.; Atwater, H. A. *Nat. Mater.* **2005**, *4*, 143.
(6) Lombardo, S.; De Salvo, B.; Gerardi, C.; Baron, T. *Microelectron. Eng.* **2004**, *72*, 388.
(7) Compagnoni, C. M.; Gusmeroli, R.; Ielmini, D.; Spinelli, A. S.; Lacaita, A. L. *J. Nanosci. Nanotech.* **2007**, *7*, 193.
(8) Erogbogbo, F.; Yong, K. T.; Roy, I.; Xu, G. X.; Prasad, P. N.; Swihart, M. T. *ACS Nano* **2008**, *2*, 873.
(9) Hessel, C. M.; Henderson, E. J.; Veinot, J. G. C. *Chem. Mater.* **2006**, *18*, 6139.
(10) Hessel, C. M.; Henderson, E. J.; Veinot, J. G. C. *J. Phys. Chem. C* **2007**, *111*, 6956.
(11) Hessel, C. M.; Henderson, E. J.; Kelly, J. A.; Cavell, R. G.; Sham, T. K.; Veinot, J. G. C. *J. Phys. Chem. C* **2008**, *112*, 14247.

Published on Web 10/22/2009

by defect annealing with extended processing.[12,13] Free-standing Si-NCs are obtained from these composites through HF etching of the SiO_2 matrix, which also enables nanocrystal size control and the tuning of the PL across the visible spectrum.

HSQ is predominantly used in the microelectronics industry as a spin-on dielectric. It is solution processable and has excellent planarization and gap-fill properties, and thin films can be applied using straightforward methods such as spin-coating.[14,15] Furthermore, sub-10 nm features can be patterned in HSQ films through electron-beam (e-beam) lithography, in which HSQ acts as a negative resist.[16] We have recently demonstrated that these films and patterns can yield luminescent oxide-embedded Si-NCs on both flat and nonflat substrates after appropriate thermal processing.[17] In such a manner, the solution processability of HSQ provides a synthetic approach to Si-NCs with unparalleled versatility, from which additional applications can be derived, including the formation of optical cavities containing Si-NCs that exhibit whispering gallery modes with high quality factors.[18]

The preparation of silsesquioxanes ($RSiO_{3/2}$, R = H, alkyl, aryl) has been extensively studied. These useful materials are typically produced by hydrolysis and condensation of an appropriate trialkoxy- or trichloro-silane (i.e., $RSi(OR')_3$, R' = alkyl; $RSiCl_3$). It is well-established that variations to synthetic conditions provides control over the structure of the silsesquioxane, including formation of random, cage, ladder, and partial cage structures.[19] It has also been reported that uncontrolled syntheses can lead to insoluble random structures.[20] Therefore, the solution processability of HSQ can be ensured through structural optimization in controlled syntheses,[19,21] such as the "scarce-water" hydrolysis originally reported by Frye and Collins.[22] In such a manner, HSQ cage structures and soluble resinous oligomers are formed, and unwanted extended polymerization is minimized. Many of these syntheses require the use of organic solvents for solubility and appropriate precursor dilution, strong acids to catalyze hydrolysis and condensation reactions and inhibit Si−H bond cleavage, as well as slow water addition (e.g., dropwise or bubbled into the reaction mixture in an inert carrier gas).[19]

For applications that do not require the solution processability of HSQ, such as the preparation of bulk quantities of SiO_2-embedded Si-NCs, it is straightforward to prepare suitable $(HSiO_{1.5})_n$ sol−gel polymers using less extensive synthetic protocols. Sol−gel chemistry is an effective method to incorporate silicon hydride (Si−H) functionalities into SiO_2-based gels, ceramics, and silicon oxicarbide glasses. Many investigations have exploited the compositional versatility of sol−gel techniques to introduce Si−H groups as a means of modifying the composition, structure, and properties of the final solids.[23−25] The majority of these syntheses employed acid-catalyzed sol−gel processing of organic solutions of Si−H containing alkoxysilanes ($HSi(OMe)_3$ or $HSi(OEt)_3$). The preparation of $(HSiO_{1.5})_n$ sol−gel homopolymers have also been evaluated as precursors for Si-NC formation, usually exploiting the sol−gel behavior of $HSi(OEt)_3$.[26−28] Similar to HSQ, appropriate thermal processing of these gels gives rise to SiO_2-embedded Si-NCs which exhibit characteristic PL emission. The sensitization of Er^{3+} by the oxide-embedded Si-NCs in these systems has also been reported.[28]

Several of the reports describing the formation of Si-NCs from $HSiO_{1.5}$ sol−gel polymers have identified the presence of uncondensed ethoxy (−OEt) groups in the final gels,[26,29] which undoubtedly modify the structure of the oxide network and most certainly influence the formation and growth of Si-NCs. For example, it was reported that ca. 10 nm diameter Si-NCs were formed after thermal processing at 700 °C.[26] This comparatively low temperature for NC formation is quite different from our observations of Si-NCs formed from HSQ, in which crystallization began at 1000 °C, and Si-NCs processed at 1100 °C exhibited average diameters of ca. 3.5 nm. Our observations are supported by similar reports for the onset of Si-NC crystallization from other $(HSiO_{1.5})_n$ precursor systems.[27] In light of the retention of network modifying −OEt functionalities in the gel resulting from incomplete condensation, it is reasonable that this difference in behavior can be attributed to a decrease in the energetic barrier to diffusion of Si atoms throughout the oxide network. In this context, Si cluster nucleation and crystallization would be facilitated, and larger Si-NCs would form at lower temperatures. This has also recently been reported for Si-NC formation in P-doped silicon-rich oxide (SRO) films.[30] Similar conclusions have been made for oxide-embedded Ge-NC formation when

(12) Cheylan, S.; Elliman, R. G. *Appl. Phys. Lett*. **2001**, *78*, 1225.
(13) Lockwood, R.; Hryciw, A.; Meldrum, A. Appl. Phys. Lett. **2006**, *89*, 263112.
(14) Loboda, M. J.; Grove, C. M.; Schneider, R. F. *J. Electrochem. Soc*. **1998**, *145*, 2861.
(15) Albrecht, M. G.; Blanchette, C. *J. Electrochem. Soc*. **1998**, *145*, 4019.
(16) Namatsu, H.; Takahashi, Y.; Yamazaki, K.; Yamaguchi, T.; Nagase, M.; Kurihara, K. *J. Vac. Sci. Tech. B* **1998**, *16*, 69.
(17) Hessel, C. M.; Summers, M. A.; Meldrum, A.; Malac, M.; Veinot, J. G. C. *Adv. Mater*. **2007**, *19*, 3513.
(18) Rodríguez, J. R.; Veinot, J. G. C.; Bianucci, P.; Meldrum, A. *Appl. Phys. Lett*. **2008**, *92*, 131119.
(19) Baney, R. H.; Itoh, M.; Sakakibara, A.; Suzuki, T. *Chem. Rev*. **1995**, *95*, 1409.
(20) Kawakami, Y. *React. Funct. Polymers* **2007**, *67*, 1137.
(21) Liu, W. C.; Yu, Y. Y.; Chen, W. C. *J. Appl. Polym. Sci*. **2004**, *91*, 2653.
(22) Frye, C. L.; Collins, W. T. *J. Am. Chem. Soc*. **1970**, *92*, 5586.
(23) Loy, D. A.; Baugher, B. M.; Baugher, C. R.; Schneider, D. A.; Rahimian, K. *Chem. Mater*. **2000**, *12*, 3624.
(24) Campostrini, R.; Sicurelli, A.; Ischia, M.; Carturan, G. *J. Therm. Anal. Calor*. **2007**, *89*, 633.
(25) Sorarù, G. D.; D'Andrea, G.; Campostrini, R.; Babonneau, F.; Mariotto, G. *J. Am. Ceram. Soc*. **1995**, *78*, 379.
(26) Pauthe, M.; Bernstein, E.; Dumas, J.; Saviot, L.; Pradel, A.; Ribes, M. *J. Mater. Chem*. **1999**, *9*, 187.
(27) Sorarã, G. D.; Modena, S.; Bettotti, P.; Das, G.; Mariotto, G.; Pavesi, L. *Appl. Phys. Lett*. **2003**, *83*, 749.
(28) Jimenez De Castro, M.; Pivin, J. C. *J. Sol-Gel Sci. Tech*. **2003**, *28*, 37.
(29) Das, G.; Ferraioli, L.; Bettotti, P.; De Angelis, F.; Mariotto, G.; Pavesi, L.; Di Fabrizio, E.; Soraru, G. D. *Thin Solid Films* **2008**, *516*, 6804.
(30) Hao, X. J.; Cho, E. C.; Scardera, G.; Bellet-Amalric, E.; Bellet, D.; Shen, Y. S.; Huang, S.; Huang, Y. D.; Conibeer, G.; Green, M. A. *Thin Solid Films* **2009**, *517*, 5646.

processed under H_2. The reduction of Ge oxides by atmospheric hydrogen produces hydroxyl (Ge−OH) groups which facilitate Ge atomic diffusion through the modified oxide network, resulting in a lower energetic barrier to crystallization.[31,32] Therefore, controlled changes in the internal structure of the diffusion-mediating oxide matrix should directly influence the formation and growth of Si-NCs from $(HSiO_{1.5})_n$ precursors.

Here, we present the preparation of SiO_2-embedded Si-NCs from $(HSiO_{1.5})_n$-based sol−gel polymers produced from the straightforward addition of water to $HSiCl_3$, focusing on the influence of the polymer structure on nanocrystal formation and growth. We demonstrate that our $(HSiO_{1.5})_n$ polymer has greater network character than HSQ arising from a higher cross-linking density, and as such, smaller Si-NCs are produced under identical processing conditions. This polymer structure/NC size relationship is further supported by the preparation of methyl-modified $(HSiO_{1.5})_n(CH_3SiO_{1.5})_m$ ($m \ll n, m+n=1$) sol−gel copolymers, in which a low concentration of methyl groups act as network modifiers and facilitate diffusion of Si atoms through the oxide network by decreasing the cross-linking density. Si-NCs formed from these copolymers are larger than those obtained from the $(HSiO_{1.5})_n$ homopolymer when processed under identical conditions. All but the largest oxide-embedded Si-NCs described herein exhibit intense PL in accordance with the principles of quantum confinement. Additionally, free-standing Si-NCs are liberated from the oxide matrix through HF etching. Materials in this investigation were characterized using Fourier transform infrared (FTIR) spectroscopy, X-ray diffraction (XRD), and photoluminescence (PL) spectroscopy.

Experimental Details

Reagents and Materials. HSQ was purchased from Dow Corning (trade name FOx) as a solution in methyl isobutyl ketone (MIBK). This stock solution was used as received, stored in subdued light and an inert atmosphere prior to use, and solid HSQ was obtained by solvent evacuation in vacuo. Trichlorosilane ($HSiCl_3$, 99%) and methyl trichlorosilane (CH_3SiCl_3, 99%) were purchased from Sigma Aldrich, stored in a nitrogen glovebox in subdued light, and used as received. Electronic grade hydrofluoric acid (49% aqueous solution, J. T. Baker), sodium chloride (caledon, 99%), hexanes (Sigma-Aldrich, ACS grade), and ethanol (95%, Sigma-Aldrich) were used as received. High-purity water (18.2 MΩ/cm) was obtained from a Barnstead Nanopure Diamond purification system.

$(HSiO_{1.5})_n$ Condensation Polymer Preparation. In a typical synthesis, 4.5 mL of $HSiCl_3$ (6.0 g, 45 mmol) was added to a round-bottom flask equipped with a magnetic stir bar and stirred in a Ar atmosphere while cooling in a water/ice bath (0 °C) using standard Schlenk techniques. The reaction mixture was cooled to minimize vapor-phase hydrolysis and condensation reactions owing to the high vapor pressure of $HSiCl_3$ (bp = 32−34 °C). Deionized (DI) water (1.59 mL, 90 mmol) was rapidly injected in one aliquot with vigorous stirring into the cooled $HSiCl_3$ through a septum. The volume of water used corresponds to a H_2O:$HSiCl_3$ molar ratio of 2:1. As the reaction produces $HCl_{(g)}$, an exhaust vent was connected to the reaction flask prior to injection of water to prevent overpressurization. Upon addition of water, the clear and colorless $HSiCl_3$ immediately reacted, forming a white precipitate. Hydrolysis of the precursor was confirmed by monitoring the pH of the reaction mixture (pH ≤ 1). The precipitate remained immersed in the acidic aqueous mixture for 30 min to ensure complete hydrolysis and condensation and was subsequently isolated and dried in vacuo. The resulting white solid $(HSiO_{1.5})_n$ polymer was obtained in yields greater than 95% and was maintained in inert atmosphere to prevent oxidation.

$(HSiO_{1.5})_n(CH_3SiO_{1.5})_m$ ($m \ll n$) Condensation Copolymer Preparation. The synthetic conditions for copolymers of $HSiCl_3$ and CH_3SiCl_3 were identical to those described for the preparation of the $(HSiO_{1.5})_n$ homopolymer from $HSiCl_3$ (vide supra). Three copolymers were synthesized with varying compositions, in which the mole percent of CH_3SiCl_3 relative to $HSiCl_3$ was 2.5%, 5%, and 10%. In addition, a $(CH_3SiO_{1.5})_n$ homopolymer was also prepared. In all cases, the volume of water was modified to maintain a H_2O:silane ratio of 2:1.

Si-NC/SiO_2 Composite Preparation. Si-NC/SiO_2 precursor (i.e., $HSQ_{(s)}$, $(HSiO_{1.5})_n$, or $(HSiO_{1.5})_n(CH_3SiO_{1.5})_m$ ($m \ll n$)) were processed similar to previous reports.[9] In brief, the white solid precursor was placed in a quartz reaction boat and transferred to a high-temperature tube furnace. During transfer, exposure to air was minimized. Samples were thermally processed in a slightly reducing (5% H_2/95% Ar) atmosphere to defined peak processing temperatures (1100−1400 °C) at 18 °C/min and maintained there for predetermined times (1 or 10 h). After cooling to room temperature, the resulting dark brown solid products were mechanically ground in an agate mortar and pestle to yield fine, free-flowing powders.

Liberation of Hydride Surface Terminated Freestanding Si-NCs. Prior to etching, additional salt grinding of the composite (2:1 mass ratio of NaCl: composite) in a mortar and pestle was performed to produce a very fine powder and to maximize particle homogeneity. Sodium chloride was subsequently removed by repeated washing and centrifugation with water, and the recovered brown powders were fully dried in an Ar stream. A representative etching procedure involved transferring 50 mg of salt-ground composite to a Teflon beaker containing 5 mL of a 1:1:1 solution of 49% $HF_{(aq)}$:H_2O:CH_3CH_2OH. The mixture was stirred for a predetermined time to etch the SiO_2 matrix and gradually decrease the size of the Si-NCs. Aliquots were taken at 35, 50, and 65 min, at which point hydrophobic, hydride-terminated freestanding Si-NCs were isolated by extraction from the aqueous solution into hexanes.

Fourier Transform Infrared Spectroscopy (FTIR). FTIR spectroscopy was performed on powder samples using a Nicolet Magna 750 IR spectrophotometer.

X-ray Powder Diffraction (XRD). XRD was performed using an INEL XRG 3000 X-ray diffractometer equipped with a Cu Kα radiation source ($\lambda = 1.54$ Å). Bulk crystallinity for all samples was evaluated on finely ground samples mounted on a low-intensity background silicon (100) sample holder.

Photoluminescence (PL) spectroscopy. PL spectra of finely powdered composites drop-coated from an ethanol suspension onto optical-grade quartz were evaluated at room temperature using the 325 nm line of a He−Cd laser excitation source. PL emission was detected with a fiber optic digital charge-coupled device (CCD) spectrometer whose spectral response

(31) Choi, W. K.; Chew, H. G.; Zheng, F.; Chim, W. K.; Foo, Y. L.; Fitzgerald, E. A. *Appl. Phys. Lett.* **2006**, *89*, 113126.
(32) Chew, H. G.; Zheng, F.; Choi, W. K.; Chim, W. K.; Foo, Y. L.; Fitzgerald, E. A. *Nanotechnology* **2007**, *18*, 065302.

Scheme 1. Hydrolysis and Condensation Reactions That Form $(HSiO_{1.5})_n$ Polymers from H-$SiCl_3$[a]

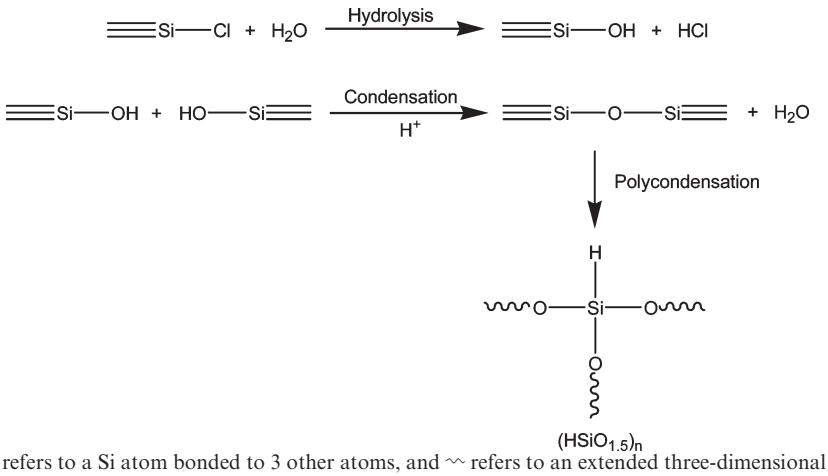

[a] In this representation, ≡ refers to a Si atom bonded to 3 other atoms, and ~ refers to an extended three-dimensional network with Si−H centers bridged by siloxane linkages (Si−O−Si).

was normalized using a standard blackbody radiator. PL spectra of hexane suspensions of freestanding Si-NCs were obtained using a Cary Eclipse Fluorimeter.

Results and Discussion

$(HSiO_{1.5})_n$ Condensation Polymer. The preparation of SiO_2-embedded Si-NCs from reductive thermal processing of sol−gel polymers derived from $HSiCl_3$ is presented. The reactions that lead to the formation of $(HSiO_{1.5})_n$ polymers from the addition of water to $HSiCl_3$ are presented in Scheme 1. Hydrolysis results from nucleophilic attack of H_2O molecules at the electron-deficient Si center, and the HCl reaction byproduct catalyzes the condensation of silanol (Si−OH) groups into siloxane (Si−O−Si) linkages. The hydrolysis and subsequent polycondensation reactions form an extended three-dimensional $(HSiO_{1.5})_n$ network, with a net Si:O ratio of 1:1.5 maintained in the final polymer. The 1:2 molar ratio of $HSiCl_3$:H_2O (45 mmol:90 mmol) used in the present synthesis provides a slight excess of H_2O to facilitate mass transport and promote acid catalyzed condensation reactions. Furthermore, in light of the equilibrium nature of hydrolysis and condensation processes, the relatively low water concentration may also facilitate a shift in the equilibria promoting formation of siloxane linkages and water as products.

The structure and composition of $(HSiO_{1.5})_n$ were investigated using FTIR spectroscopy (Figure 1A). The spectrum is characterized by a sharp Si−H stretching vibration at ca. 2255 cm^{-1}, intense Si−O−Si vibrations at ca. 1000−1300 cm^{-1}, and H−Si−O hybrid vibrations at 800−900 cm^{-1}. Similar FTIR spectra have been reported for HSQ and other $(HSiO_{1.5})_n$ networks.[14,15,24] The absence of hydroxyl (−OH) stretching at ca. 3400 cm^{-1} is an indication of complete condensation reactions. It is interesting to consider the structure of the Si−O−Si and H−Si−O vibrational bands, which consist of two separate components. Previous reports outlining the thermal transformations of HSQ have identified the high frequency component of these bands (ca. 1160 cm^{-1} for Si−O−Si and ca. 875 cm^{-1} for H−Si−O) as vibrations in

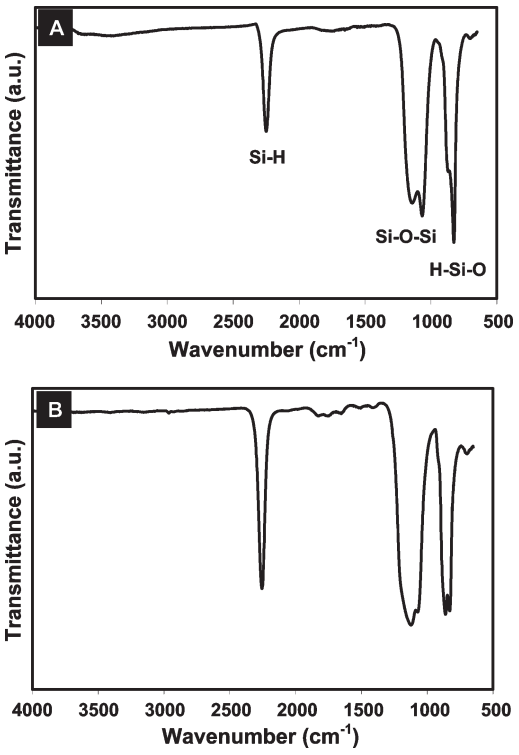

Figure 1. Fourier transform infrared (FTIR) spectrum of (A) $(HSiO_{1.5})_n$ polymer prepared by hydrolysis and condensation of $HSiCl_3$ and (B) HSQ, showing Si−H stretching, Si−O−Si stretching, and H−Si−O hybrid stretching. The structure of the Si−O−Si and H−Si−O stretching bands in the FTIR spectrum of $(HSiO_{1.5})_n$ polymer is indicative of a greater extended network structure relative to HSQ.

the cagelike structure of HSQ, while the lower frequency components (ca. 1075 cm^{-1} for Si−O−Si and ca. 830 cm^{-1} for H−Si−O) have been identified with vibrations of an extended network structure.[14,33] These assignments were attributed to slightly smaller bond angles expected for the extended network structure, in light of observations from single crystal X-ray diffraction analysis of molecular polyhedral silsesquioxanes.[34] Compared to the FTIR

(33) Yang, C. C.; Chen, W. C. *J. Mater. Chem.* **2002**, *12*, 1138.
(34) Agaskar, P. A.; Day, V. W.; Klemperer, W. G. *J. Am. Chem. Soc.* **1987**, *109*, 5554.

spectrum of HSQ (Figure 1B), which exhibits a greater intensity for vibrations associated with a cagelike structure, the $(HSiO_{1.5})_n$ polymer prepared herein shows a greater network character. This observation indicates the preparation of an extended cross-linked network in the present synthesis and is reasonable given no deliberate experimental strategies were employed to favor the cage structure.

A further comparison of the FTIR spectra of the $(HSiO_{1.5})_n$ polymer and HSQ (Figures 1A and B) reveals that the intensity of the Si−H vibration in HSQ is greater for the $(HSiO_{1.5})_n$ polymer. Although a decrease in intensity of Si−H absorbance in FTIR spectroscopy is often interpreted as a decrease in the Si−H concentration resulting from oxidation and a shift in the $SiO_{1.5}$ composition toward SiO_2, this is not always the case. In the study of the Staebler−Wronski effect in amorphous Si:H photovoltaics, it is well understood that reversible photoinduced dangling bond formation decreases the performance of the amorphous Si devices, often described by the hydrogen bond switching model.[35] However, recent advancements in the understanding of this effect have identified deficiencies in this theory, leading to several proposals to account for them. In particular, it has been proposed that photoinduced structural changes in the Si network could play a significant role.[35−37] In the context of the present investigation, it was proposed that such structural changes increase the "effective bond charge" of the Si−H bond due to local field changes, increasing the oscillator strength of the stretching vibration as a result.[37−39] Consequently, an increase in the intensity of the Si−H stretching mode was observed, without a corresponding increase in the concentration of Si−H species. Similar considerations are well-established in the study of hydrogenated SiN_x:H.[40] Given the stability of Si−H bonds in acidic aqueous environments, it is reasonable the $SiO_{1.5}$ composition was maintained in the present $(HSiO_{1.5})_n$ polymer, and the difference in the relative intensity of the Si−H stretching compared to HSQ arises from the aforementioned siloxane network structural differences.

The formation and growth of Si-NCs from $(HSiO_{1.5})_n$ was monitored using XRD. Figure 2 shows XRD patterns of $(HSiO_{1.5})_n$ processed at 1100, 1200, and 1400 °C for 1 h along with samples of HSQ processed under identical conditions. For $(HSiO_{1.5})_n$ processed at 1100 °C, the appearance of broad reflections at ca. 28°, 47°, and 56° that are readily indexed to the (111), (220), and (311) crystal planes of diamond structure Si is indicative of the formation of Si-NCs. Increasing the processing temperature

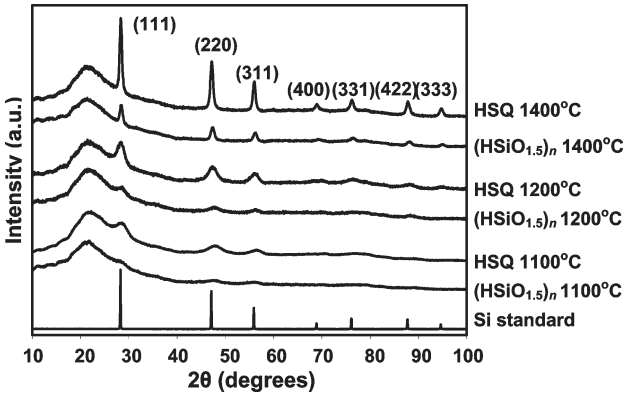

Figure 2. X-ray diffraction (XRD) patterns of $(HSiO_{1.5})_n$ and HSQ thermally processed at 1100, 1200, and 1400 °C for 1 h in 5% H_2/95% Ar showing the influence of processing temperature on Si-NC growth. An XRD pattern of a Si standard is included for comparison.

to 1400 °C leads to an increased intensity and narrowing of these reflections as well as the emergence of higher order crystal planes—all indicative of nanocrystal growth. These observations demonstrate that SiO_2-embedded Si-NCs are readily formed from $(HSiO_{1.5})_n$ sol−gel polymers, and variations to peak processing temperature is a convenient method for nanocrystal size tuning.

In comparison to Si-NC/SiO_2 composite samples obtained from HSQ under identical conditions (Figure 2), it is evident that $(HSiO_{1.5})_n$ derived samples show broader lower intensity reflections. This observation indicates smaller Si-NCs form upon processing $(HSiO_{1.5})_n$. Scherrer analysis of XRD peak broadening for samples processed at 1200 °C gave estimated average diameters of ca. 4 and 4.5 nm for $(HSiO_{1.5})_n$ and HSQ, respectively. Similar analyses of samples processed at 1400 °C gave estimated average nanocrystal diameters of ca. 10 and 13 nm for $(HSiO_{1.5})_n$ and HSQ, respectively. Comparative Scherrer analyses for samples processed at 1100 °C was not possible due to the low intensity of the crystalline Si reflections relative to the amorphous oxide background.

While the disparity in Si-NC size obtained from $(HSiO_{1.5})_n$ and HSQ could result from differences in both the composition and structure of these precursors, substantial compositional differences are unlikely given the stability of Si−H in acidic aqueous environments and the identical handling of the precursors. As previously described, analysis of FTIR spectra (vide supra) revealed that $(HSiO_{1.5})_n$ possesses more network character than HSQ. As a result, it is reasonable that Si diffusion through the more cross-linked network of $(HSiO_{1.5})_n$ is more energetically demanding and would thus hinder the formation and growth of Si-NCs. Similar conclusions regarding diffusion effects on the formation and growth of semiconductor nanocrystals in network-modified matrices have been reported.[30−32]

Similar to size-controlled Si-NCs prepared by the thermal processing of HSQ, those formed from the present $(HSiO_{1.5})_n$ condensation polymers also exhibit size-dependent PL in accordance with the principles of quantum confinement (Figure 3A). As the peak thermal processing temperature is increased from 1100 to 1200 °C,

(35) Kolodziej, A. *Opto-Elect. Rev.* **2004**, *12*, 21.
(36) Kong, G. L.; Zhang, D. L.; Yue, G. Z.; Wang, Y. Q.; Liao, X. B. *Proc. Mater. Res. Soc. Symp.* **1999**, *507*, 697.
(37) Fritzsche, H. *Solid State Commun.* **1995**, *94*, 953.
(38) Brodsky, M. H.; Cardona, M.; Cuomo, J. J. *Phys. Rev. B* **1977**, *16*, 3556.
(39) John, P.; Odeh, I. M.; Thomas, M. J. K.; Tricker, M. J.; Wilson, J. I. B.; England, J. B. A.; Newton, D. *J. Phys. C: Solid State Physics* **1981**, *14*, 309.
(40) Verlaan, V.; Van Der Werf, C. H. M.; Arnoldbik, W. M.; Goldbach, H. D.; Schropp, R. E. I. Phys. Rev. B **2006**, *73*, 195333.

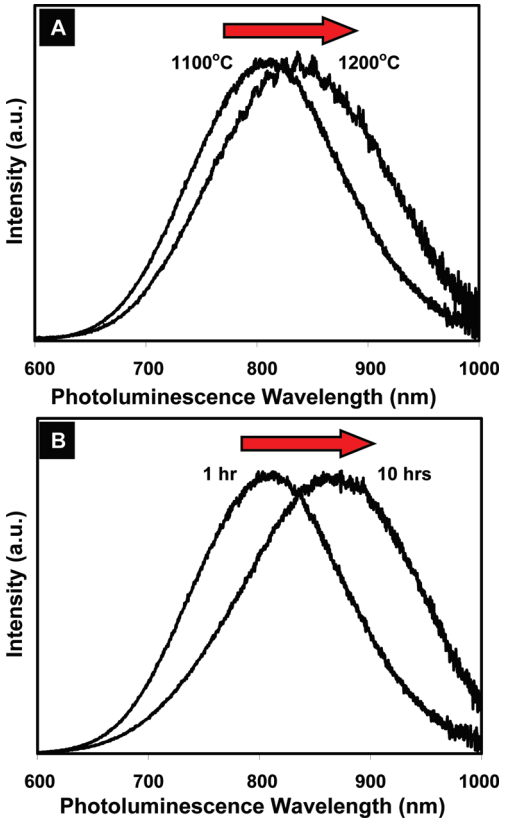

Figure 3. (A) Normalized photoluminescence (PL) spectra of SiO_2-embedded Si-NCs produced from $(HSiO_{1.5})_n$ showing the effect of peak thermal processing temperature in 5% H_2/95% Ar. (B) Normalized photoluminescence (PL) spectra of SiO_2-embedded Si-NCs produced from $(HSiO_{1.5})_n$ showing the effect of extended thermal processing at 1100 °C in 5% H_2/95% Ar.

the PL maximum red shifts from ca. 810 to 830 nm. This is expected in light of the observed trend in XRD peak broadening with increased processing temperature (vide supra). Samples processed at 1400 °C did not exhibit PL, likely a result of their relatively large diameters (10 nm) which are greater than the Bohr exciton radius. In contrast, Si-NCs produced from HSQ under identical conditions exhibit PL centered at ca. 825 and 840 nm for 1100 and 1200 °C, respectively.[10] In quantum confined emission, longer wavelength (i.e., lower energy) PL is indicative of larger nanocrystal size, consistent with the present XRD observations (vide supra).

The effect of extended thermal processing time on the PL behavior of Si-NCs produced from $(HSiO_{1.5})_n$ polymer was also investigated (Figure 3B). As processing time is increased from 1 to 10 h at 1100 °C, the PL red shifts from ca. 810 to 870 nm. This observation has previously been attributed to nonresonant carrier tunneling to larger nanocrystals upon defect passivation during thermal annealing.[13] However, the larger Si-NCs produced from HSQ under identical conditions exhibit longer wavelength emission.[10]

It has been shown that $(HSiO_{1.5})_n$ sol−gel polymers produced by the straightforward addition of water to $HSiCl_3$ are efficient cost-effective precursors for the synthesis of SiO_2-embedded and freestanding Si-NCs. Dimensional differences of Si-NCs obtained from HSQ under identical processing conditions have been attributed to the greater

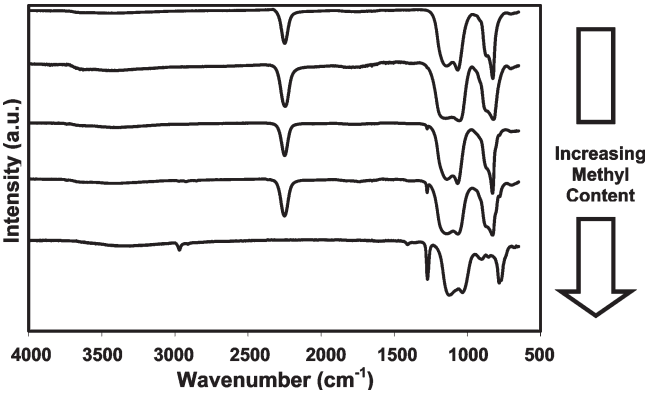

Figure 4. Fourier transform infrared (FTIR) spectra of compositionally tuned $(HSiO_{1.5})_n(CH_3SiO_{1.5})_m$ condensation copolymers ($m = 2.5, 5, 10\%$), showing a monotonic increase in $-CH_3$ bending (ca. 1260 cm^{-1}) and C−H stretching (ca. 2900 cm^{-1}) as the concentration of methyl groups in the copolymers increases. Spectra for $(HSiO_{1.5})_n$ (0%) and $(CH_3SiO_{1.5})_n$ (100%) homopolymers are included for comparison.

network character of $(HSiO_{1.5})_n$. This higher degree of cross-linking imparts a larger diffusion barrier to Si atoms during thermally induced redistribution reactions. As a result, smaller nanocrystals are produced, and their PL is slightly blue-shifted in accordance with quantum confinement. To verify this proposal, analogous sol−gel copolymers were investigated in which small concentrations of network modifying Si−CH_3 groups were included. It is our proposal that these methyl groups act to decrease the overall sol−gel cross-linking density, opening the network, and facilitating Si atomic mobility during thermal processing. Consequently, larger Si-NCs should be formed in comparison to the $(HSiO_{1.5})_n$ homopolymer.

$(HSiO_{1.5})_n(CH_3SiO_{1.5})_m$ ($m \ll n$) Condensation Copolymers. To further investigate the role of the $(HSiO_{1.5})_n$ polymeric network internal structure in the formation of Si-NCs upon thermal processing, a series of condensation copolymers were prepared containing defined concentrations of Si−CH_3 groups. We expect the greater steric bulk of the methyl-substituents (Si−CH_3) to decrease the overall cross-linking density of the polymeric network. Copolymers with CH_3/H molar ratios of 2.5% (i.e., $[(HSiO_{1.5})_{0.975}(CH_3SiO_{1.5})_{0.025}]_n$), 5% (i.e., $[(HSiO_{1.5})_{0.95}(CH_3SiO_{1.5})_{0.05}]_n$), and 10% (i.e., $[(HSiO_{1.5})_{0.90}(CH_3SiO_{1.5})_{0.10}]_n$) were prepared by varying the relative concentrations of $HSiCl_3$ and CH_3SiCl_3 in the hydrolysis and condensation mixtures prior to addition of water.

The FTIR spectra of the as-prepared $(HSiO_{1.5})_n(CH_3SiO_{1.5})_m$ condensation copolymers are presented in Figure 4. Spectra of $(HSiO_{1.5})_n$ and $(CH_3SiO_{1.5})_n$ homopolymers are included for comparison. All copolymers investigated here retain Si−H groups during hydrolysis and condensation, as evidenced by the strong Si−H stretching vibration at ca. 2255 cm^{-1}. The increase in Si−CH_3 concentration in the compositionally tuned copolymers is manifested in the monotonic increase of the $-CH_3$ symmetric bending vibration (ca. 1260 cm^{-1}) and C−H stretching (ca. 2900 cm^{-1}) intensities.[41] These observations

(41) Xiao, D.; Zhang, H.; Wirth, M. *Langmuir* **2002**, *18*, 9971.

indicate that the relative concentrations of the $HSiCl_3$ and CH_3SiCl_3 precursors in the reaction mixture were maintained in the condensation copolymers.

Recall, structural differences between HSQ and $(HSiO_{1.5})_n$ were extracted from the structure of the Si−O−Si and H−Si−O vibrational bands in their FTIR spectra (vide supra), with the higher energy component of each band associated with cagelike character, and the lower energy component with network character. Comparisons of these two materials are possible because both precursors possess the same composition. Similar analyses have been reported for the structural evolution of methyl silsesquioxane systems.[42] However, for the present copolymers, compositional differences make similar interpretations nontrivial, with overlapping absorption bands and the possibility of phase segregation complicating the analysis.[21]

The effect of methyl concentration on the formation of Si-NCs during thermal processing of compositionally tuned $(HSiO_{1.5})_n(CH_3SiO_{1.5})_m$ copolymers was evaluated by heating all precursors at 1100 °C for 1 h in 5% H_2/95% Ar. The XRD patterns of Si-NC/SiO_2 composites obtained from these copolymers differ from those obtained from the $(HSiO_{1.5})_n$ homopolymer (Figure 5). All samples contain Si-NCs, as evidenced by the broad reflections characteristic of diamond structure Si. As the methyl concentration in the $(HSiO_{1.5})_n(CH_3SiO_{1.5})_m$ copolymers is increased from 0 to 5%, these reflections narrow and intensify, indicative of larger Si-NCs. Scherrer analysis of XRD peak broadening of the sample prepared from $[(HSiO_{1.5})_{0.95}(CH_3SiO_{1.5})_{0.05}]_n$ (i.e., 5% CH_3/H) yielded an estimated average nanocrystal diameter of ca. 4.5 nm. In fact, these Si-NCs are larger than those obtained from processing the $(HSiO_{1.5})_n$ homopolymer at 1200 °C (vide supra). Since these samples were processed under identical conditions, this increased nanocrystal growth is a direct result of $-CH_3$ group incorporation into the polymeric network.

PL spectra (Figure 6) exhibit a red shift in the emission maximum with higher methyl concentration in the copolymers, with a peak maximum centered at ca. 875 nm for $[(HSiO_{1.5})_{0.95}(CH_3SiO_{1.5})_{0.05}]_n$ (i.e., 5% CH_3/H). This behavior agrees with our interpretation of the present XRD data—Si-NC size increases with greater methyl concentration in the copolymer precursor (vide supra).

Clearly, incorporating low concentrations of network-modifying methyl substituents into $(HSiO_{1.5})_n(CH_3SiO_{1.5})_m$ condensation copolymers influences the formation of SiO_2-embedded Si-NCs upon reductive thermal processing. In agreement with our conclusions regarding the difference in nanocrystal formation from HSQ and $(HSiO_{1.5})_n$, the structure of the polymer network and the overall cross-linking density plays an important role in the evolution of the Si-NCs. "Opening up" the siloxane network through $-CH_3$ incorporation facilitates Si atomic diffusion, and more atoms can contribute to nanocrystal formation and growth. This is directly supported by XRD observations that showed reflection narrowing attributed to increased Si-NC size as the methyl concentration in the copolymers was increased from 0 to 5%. Further evidence was obtained by PL spectroscopy that showed a red shift in the emission with greater methyl content, in agreement with quantum confined emission in Si-NCs of increasing size.

Although the data presented here does not directly demonstrate structural control due to the limitations previously mentioned regarding the interpretation of FTIR spectra of $(HSiO_{1.5})_n(CH_3SiO_{1.5})_m$ copolymers (vide supra), additional support for the present conclusions can be obtained by considering compositional effects. During thermal processing of organically modified siloxane polymers, including the $(HSiO_{1.5})_n(CH_3SiO_{1.5})_m$ condensation copolymers presented here, carbon atoms are retained in the final oxide network, bonded to silicon in oxycarbide phases.[25] As a result, these silicon atoms are unavailable to participate in the formation and

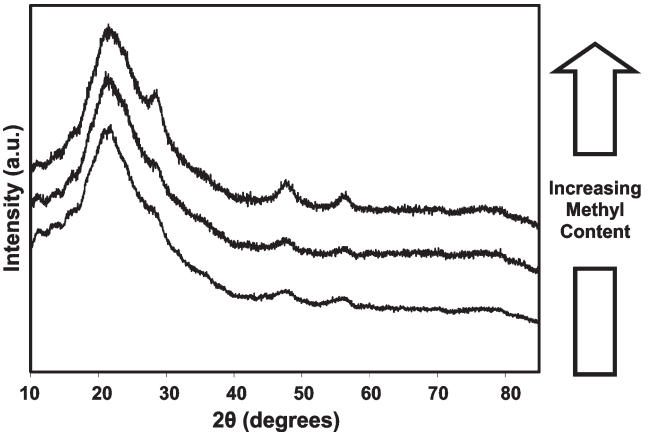

Figure 5. X-ray diffraction (XRD) patterns of compositionally tuned $(HSiO_{1.5})_n(CH_3SiO_{1.5})_m$ condensation copolymers (m = 0, 2.5, 5%) thermally processed at 1100 °C for 1 h in 5% H_2/95% Ar, showing the relationship between Si-NC size and methyl concentration in the copolymer.

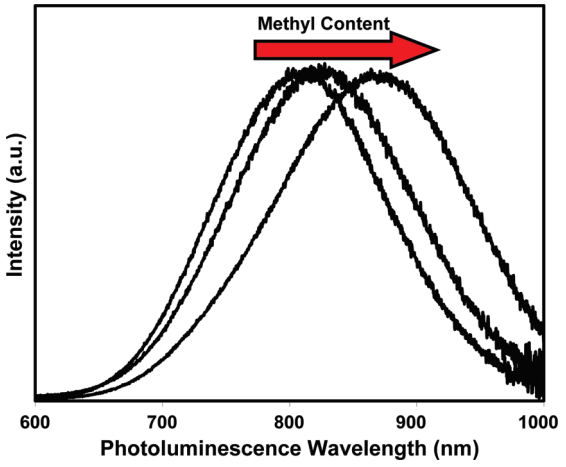

Figure 6. Normalized photoluminescence (PL) spectra of compositionally tuned $(HSiO_{1.5})_n(CH_3SiO_{1.5})_m$ condensation copolymers (m = 0, 2.5, 5%) thermally processed at 1100 °C for 1 h in 5% H_2/95% Ar, showing the relationship between PL maximum and methyl concentration in the copolymers.

(42) Lee, L. H.; Chen, W. C.; Liu, W. C. *J. Polym. Sci., Part A: Polym. Chem.* **2002**, *40*, 1560.

growth of Si-NCs. This can be described as a depletion of Si in the SRO and a shift from the original $SiO_{1.5}$ composition of $(HSiO_{1.5})_n$ toward SiO_2. Consequently, this compositional shift is expected to lead to smaller Si-NCs and a blue shift in their PL emission.[43] This is opposite to what is observed for the present compositionally tuned $(HSiO_{1.5})_n(CH_3SiO_{1.5})_m$ copolymers. Therefore, even though compositional changes brought about by $-CH_3$ incorporation would be expected to produce smaller Si-NCs, the effects of these methyl substituents on the internal structure of the polymer network and the diffusion of Si atoms through the matrix dominate, leading to an increase in Si-NC size.

Thermal processing of the $[(HSiO_{1.5})_{0.90}(CH_3SiO_{1.5})_{0.10}]_n$ copolymer (i.e., 10% CH_3/H), however, did not result in the expected increase in Si-NC size and PL red-shift. Instead, the XRD pattern and PL spectrum (not shown) were very similar to analogous samples prepared from the $(HSiO_{1.5})_n$ homopolymer, although the intensity of the XRD reflections was slightly lower. Additionally, thermal processing of the $(CH_3SiO_{1.5})_n$ homopolymer resulted in no evident Si-NC formation by XRD and PL characterization, as expected with the formation of silicon oxycarbide phases. Therefore, at 10% CH_3/H, compositional effects become more important than structural effects, and the associated decrease in available Si atoms leads to smaller Si-NCs. This balance between compositional and structural effects on the formation of SiO_2-embedded Si-NCs suggests that a limit exists for the applicability of methyl-modified copolymers in obtaining the largest possible nanocrystals at the lowest possible temperature. To this end, we are currently extending this investigation into other copolymer systems, including the incorporation of bulkier substituents and the use of dichlorosilanes ($SiCl_2RR'$; R, R′ = H, alkyl, aryl) as network modifiers.

Freestanding Si-NCs from $(HSiO_{1.5})_n$ Sol−Gel Polymers. Si-NCs produced from thermal processing of $(HSiO_{1.5})_n$ are also suitable for applications where freestanding nanocrystals are required. Etching of SiO_2-embedded Si-NCs with aqueous HF solutions is an effective method for liberating the nanocrystals from the encapsulating oxide. Furthermore, the etching procedure provides a straightforward method to further control the diameter of the freestanding Si-NCs. The etching time dependence of the PL spectra of hydride-surface terminated Si-NCs is shown in Figure 7. All freestanding Si-NCs were liberated from $(HSiO_{1.5})_n$-derived composites processed at 1100 °C for 1 h in 5% H_2/95% Ar. Freestanding Si-NCs produced by this method exhibit intense room-temperature visible PL. Prolonged exposure to HF leads to a gradual decrease in Si-NC size and a blue shift in PL emission, as expected from quantum confinement.

A representative FTIR spectrum of fully etched, hydride-terminated Si-NCs is shown in Figure 8. The

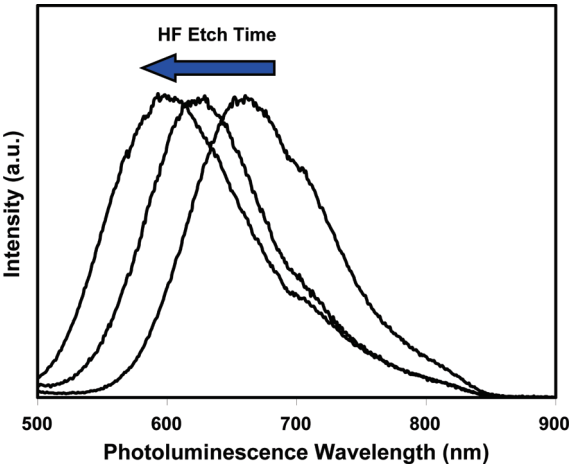

Figure 7. Normalized photoluminescence (PL) spectra of size-controlled freestanding Si-NCs produced from $(HSiO_{1.5})_n$ processed at 1100 °C for 1 h in 5% H_2/95% Ar as a function of HF etching time (35, 50, and 65 min). The blue-shift with decreasing Si-NC diameter is in accordance with quantum confinement.

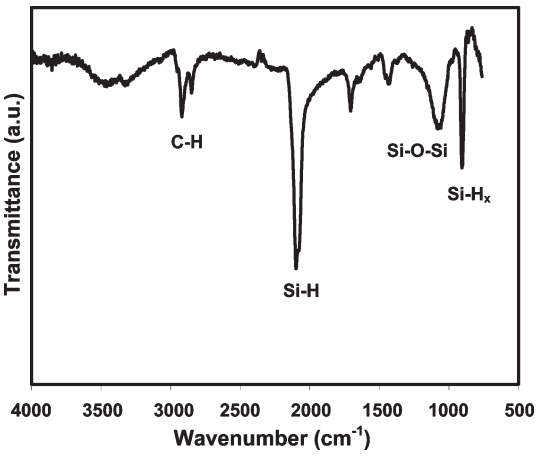

Figure 8. FTIR spectrum of freestanding Si-NCs produced from $(HSiO_{1.5})_n$ clearly showing Si−H surface termination resulting from HF etching (65 min).

freestanding Si-NCs have Si−H surface termination, as evidenced by the characteristic stretching and scissoring frequencies at ca. 2100 and 910 cm^{-1}, respectively. Hydride-surface termination is a versatile reaction platform for subsequent derivatization via hydrosilylation reactions with terminal alkenes.[44,45] Weak Si−O−Si stretching at ca. 1100 cm^{-1} and O−H stretching centered at ca. 3400 cm^{-1} arise due to limited postetching surface oxidation. Residual hexane from the extraction of Si-NCs from the aqueous etching mixture gives rise to minor C−H stretching. The impact of structural and compositional effects in these $(HSiO_{1.5})_n$ and $[(HSiO_{1.5})_n(CH_3SiO_{1.5})_m]$ sol−gel polymers on the etching of the resulting Si-NC/SiO_2 composites is a topic of ongoing investigation in our laboratory.

Conclusion

We have shown that $(HSiO_{1.5})_n$ sol−gel polymers, produced by the straightforward addition of water to

(43) Meldrum, A.; Hryciw, A.; MacDonald, A. N.; Blois, C.; Marsh, K.; Wang, J.; Li, Q. *J. Vac. Sci. Tech. A* **2006**, *24*, 713.
(44) Buriak, J. M. *Chem. Rev.* **2002**, *102*, 1271.
(45) Veinot, J. G. C. *Chem. Commun.* **2006**, 4160.

$HSiCl_3$, are efficient cost-effective precursors for the formation of SiO_2-embedded and freestanding Si-NCs. The influence of polymer structure and cross-linking density on the formation of Si-NCs was investigated by comparing samples produced from $(HSiO_{1.5})_n$ and HSQ processed under identical conditions. It was concluded that the greater network character and cross-linking density of $(HSiO_{1.5})_n$, as opposed to the cage structure characteristic of HSQ, increased the energetic requirements for Si diffusion through the oxide matrix, thereby forming smaller Si-NCs. This proposal was supported through an investigation into the formation of Si-NCs from $(HSiO_{1.5})_n(CH_3SiO_{1.5})_m$ condensation copolymers, in which methyl substituents act as network modifiers and increase Si diffusion. As such, copolymers with greater methyl concentration produced larger Si-NCs. This presents an additional method to Si-NC size control and may eventually offer the possibility of preparing larger Si-NCs at lower processing temperatures.

Acknowledgment. The authors acknowledge funding from the Natural Sciences and Engineering Research Council of Canada (NSERC), Canada Foundation for Innovation (CFI), Alberta Science and Research Investment Program (ASRIP), and University of Alberta Department of Chemistry. C. W. Moffat is thanked for assistance with FTIR spectroscopy. Dr. A. Meldrum and J. Rodríguez are thanked for assistance with laser-based photoluminescence spectroscopy. Dr. M. Fleischauer is thanked for assistance with sample characterization. J. Rodríguez, Dr. R. Clark, and T. Telesco are thanked for useful discussions.